Estrogen deficiency induces bone loss by increasing T cell proliferation and lifespan through IFN-γ-induced class II transactivator

Simone Cenci*†, Gianluca Toraldo‡, M. Neale Weitzmann*, Cristiana Roggia*, Yuhao Gao*, Wei Ping Qian*‡, Oscar Sierra‡, and Roberto Pacifici*§

*Division of Endocrinology and Metabolism, Emory University School of Medicine, Atlanta, GA 30322; †DiBiT, San Raffaele Scientific Institute, Milan 20132, Italy; and ‡Division of Bone and Mineral Diseases, Washington University School of Medicine and Barnes-Jewish Hospital, St. Louis, MO 63110

Expansion of the pool of tumor necrosis factor (TNF)-α-producing T cells is instrumental for the bone loss induced by estrogen deficiency, but the responsible mechanism is unknown. Here we show that ovariectomy up-regulates IFN-γ-induced class II transactivator, a multitarget immune modulator, resulting in increased antigen presentation by macrophages, enhanced T cell activation, and prolonged lifespan of active T cells. Up-regulation of class II transactivator derives from increased production of IFN-γ by T helper 1 cells, resulting from enhanced secretion of IL-12 and IL-18 by macrophages. The resulting T cell expansion and bone loss are prevented *in vivo* by both blockade of antigen presenting cell-induced T cell activation, and silencing of IFN-γ receptor signaling. Thus, increased IFN-γ-induced class II transactivator expression and the resulting enhanced T cell proliferation and lifespan are critical to the bone wasting effect of estrogen deficiency.

ovariectomy | osteoporosis | tumor necrosis factor | sex steroids

Estrogen deficiency causes osteoporosis, a major source of morbidity and disability in the occidental world (1). Genotropic and nongenotropic effects of estrogen lead to preservation of bone mass through modulation of bone cell lifespan (2) and decreased cytokine-driven osteoclastogenesis (3). Among the factors that up-regulate osteoclast formation in estroprevic humans and rodents is tumor necrosis factor α (TNF), a cytokine known to augment the production and the activity of the osteoclastogenic molecule RANKL (4, 5), and to potently induce IL-1, IL-6, and macrophage colony-stimulating factor, estrogen-regulated cytokines known to mediate the bone loss induced by ovariectomy (ovx) (5). Enhanced T cell production of TNF resulting from increased T cell number in the bone marrow (BM) is known to occur and to be necessary for the increase in osteoclast and the bone waste induced by ovx (6, 7). The mechanism by which ovx expands the pool of BM T cells is, however, unknown.

To address this issue we investigated the effect of estrogen deficiency on generation and death of cytokine-producing T cells. Our *in vivo* studies reveal that estrogen deficiency increases T cell activation-induced proliferation, and suppresses apoptosis of active T cells, through IFN-γ-mediated induction of the multitarget immune modulator class II transactivator (CIITA), in antigen (Ag)-presenting cells (APC) and T lymphocytes.

Methods

Mice and Surgery. All animal procedures were approved by the Institutional Animal Care and Use Committee. In all studies, female mice were sham operated or ovariectomized (ovx) at 12 weeks of age as described (8). Except for APC assays and studies with transgenic mice, C57BL/6 wild-type (WT) animals were used (Taconic, Germantown, NY). DO11.10 mice (BALB/c background) were injected i.p. with 10 mg of ovalbumin and 250 μl of complete Freund's adjuvant, as described (9), at surgery and 15 days later. BALB/c mice, DO11.10 (BALB/c), IFN-γ

receptor-deficient (IFN-γR⁻/⁻) mice and their WT littermates (129/sv) were obtained from The Jackson Laboratory.

Cell Purification. Spleen, lymph node, and BM T cells (CD90+ and CD4⁺), splenic B cells (CD19+), and BM macrophages (Mφ) (CD11b+) were purified by immunomagnetic positive selection. Lymph node dendritic cells (DC) were purified by immunomagnetic negative selection of CD19+, CD90+, and CD11b+ cells. Peritoneal Mφ were prepared by injection of 3% thioglycolate (1.5 ml per mouse), 5 days before death and retrieval (10). In each experimental group cells were purified from pools derived from at least five mice 4 weeks after surgery.

APC Assay and MHC Class II (MHCII) Expression. To test APC activity, we measured proliferation of target T cells from DO11.10 mice, prepared as follows: splenocytes from 10-week-old DO11.10 transgenic BALB/c mice were cultured in presence of ovalbumin (500 mg/ml); after 3 days, cells were passed and stimulated with IL-2 (40 units/ml) for 4 days, washed, and rested for 3 days. Sensitized and purified T cells were then incubated with APCs to be tested. Unfractionated spleen cells, purified B cells, DC, and Mφ prepared from sham-operated or ovx WT BALB/c mice 2 weeks after surgery were irradiated (2,000 γ-rad), seeded in 96-well plates (5 × 10⁵ cells per 200 μl per well) with DO11.10 T cells (APC/T cells ratio 10:1) in RPMI medium 1640 supplemented with 10% FBS, and stimulated with ovalbumin (500 mg/ml) for 56 h. APC activity was assessed by incorporation of [³H]thymidine (added at 0.5 μCi per well for the last 18 h; 1 Ci = 37 GBq). MHCII expression was detected by fluorescence-activated cell sorting (FACS) by using phycoerythrin (PE)-conjugated anti I-A/E Ab and FITC-conjugated anti-CD11b, CD11c, and CD19 Abs. All fluorochrome-conjugated Abs were provided by BD PharMingen (San Diego). In all flow cytometry experiments, acquisition and analysis were performed with FACS Calibur and CELLQUEST PRO software (BD Biosciences, San Jose, CA). Mφ were stimulated with recombinant murine IFN-γ (300 units/ml).

T Cell Proliferation, Activation, and Apoptosis. T cell proliferation was assessed by *in vivo* incorporation of BrdUrd. Briefly, sham and ovx mice were injected i.p. with BrdUrd (1 mg per 100 μl of PBS per mouse) 25 days after surgery, 72 h before death. After red cell osmotic lysis, BM cells were labeled with PE-conjugated anti-CD3 antibody (PharMingen), permeabilized with Cytofix/Cytoperm reagent (PharMingen), treated with DNase, and labeled with FITC-conjugated anti-BrdUrd (PharMingen) and

MEDICAL SCIENCES

7-amino-actinomycin D (7-AAD), according to the manufacturer's instructions. For FACS analysis, gated CD3+ cells were plotted for BrdUrd incorporation and total DNA content (7-AAD). T cell activation was measured by FACS in unfractionated BM and spleen cells stained with FITC-anti CD3 Ab and PE-anti CD25 or CD69 Abs (PharMingen). Activation and stress-induced apoptosis was analyzed by FACS as follows: purified CD4$^+$ cells were either activated with phorbol-12-myristate-13-acetate and ionomycin (both at 10 ng/ml, Sigma) or irradiated (3,000 γ-rad), and stained with FITC-Annexin V (PharMingen) and propidium iodide (PI). Annexin V+, PI− cells were counted as apoptotic. FasL expression was detected by FACS using conjugated Abs recognizing FasL (MFL3, PharMingen).

T Cell and Mϕ Cytokine Production. IFN-γ, IL-12, and IL-18 were assessed by ELISA (Quantikine, R & D Systems) in the supernatants of purified BM CD90+ and CD4$^+$ T cells (10^6 cells per ml per well), and CD11b+ Mϕ, cultured for 72 h. Cells were either left untreated or treated for the entire culture period with 17β estradiol (10 nM), cyclosporin A (100 ng/ml, Sigma), or SB203580 (5 μM, Calbiochem). T helper (T$_H$) production of IFN-γ and TNF *in vivo* was measured by FACS analysis of BM, spleen, and lymph node cells stained with PE or FITC-labeled mAbs reactive to surface CD4 and intracellular IFN-γ or TNF, on permeabilization (PharMingen).

Reverse Transcriptase Real-Time PCR. Total cytoplasmic RNA preparation and reverse transcription were conducted as described (11). Samples were analyzed by real-time PCR using a GeneAmp 5700 system (Applied Biosystems, Foster City, CA) and the following primers for CIITA: forward, 5′-AGGTTGTCAGT-GACTGCAGGC-3′; reverse, 5′-GCACAGCGACCACCT-GTGT-3′. Beta-tubulin served as the normalizing control (forward, 5′-GGAGAGCTGTGATTGCCTGC-3′; reverse, 5′-CCACCCAGTGAGTGGGTCAG-3′). The reaction was carried out in a final volume of 50 μl containing 25 μl of 0SYBR Green master mix (P/N 4304886, PE Biosystems), 20 μl of primers, and 5 μl of cDNA, for 40 cycles. Each cycle consisted of 15 sec at 95°C and 1 min at 60°C. Analysis was performed by the $\Delta\Delta$Ct method (PE Biosystems). Ct (cycle threshold) indicates the first PCR cycle at which an increase in reporter fluorescence above baseline can be detected. Fold change in mRNA is calculated as $2^{-\Delta\Delta CT}$. $\Delta\Delta CT = (Ct_{CIITA:ovx} - Ct_{tubulin:ovx}) - (Ct_{CIITA:sham} - Ct_{tubulin:sham})$, where subscripts refer to mRNA amplified (CIITA or β-tubulin) and group of study (sham or ovx).

Bone Mineral Density (BMD) Measurements and Bone Histology. Femoral BMD was determined *in vivo* at baseline and 2 and 4 weeks after surgery by using a PIXImus2 scanner (Lunar, Madison, WI). Data points represent average of both femurs for each mouse. The short-term reproducibility of this technique was 1.7%. For bone histology, left tibiae were excised, fixed in 10% formalin, decalcified, dehydrated, paraffin-embedded, sectioned, and stained with hematoxylin and for tartrate-resistant acid phosphatase activity, as described (8).

Statistical Analysis. Group mean values were compared by two-tailed Student's *t* test or ANOVA and Fisher protected lease squares difference test, as appropriate. Nondetectable vs. detectable cytokine levels were compared by Fisher exact test.

Results

Ovx Increases T Cell Activation and Lifespan of Activated T Cells. *In vivo* BrdUrd incorporation studies conducted to determine how estrogen deficiency up-regulates BM T cell number revealed that ovx increases proliferation and decreases apoptosis of T cells (Fig. 1a), two mechanisms that may be responsible for the T cell expansion induced by estrogen withdrawal. T cell proliferation is typically induced by activation. FACS analysis of the activation markers CD25 and CD69 showed that ovx increases the frequency of active T cells in the BM $\approx$2-fold (Fig. 1b), suggesting that increased proliferation is activation-dependent.

Because Ag presentation by APC is key in the regulation of T cell activation, we examined the effect of ovx on different APC lineages. Ovx increases $\approx$2-fold APC activity of spleen cells, a source of MHCII+ professional APCs of multiple lineages, as assessed by proliferation of target T cells (Fig. 1c). Analysis of subpopulations of APCs revealed that ovx specifically increases APC activity of Mϕ, but not that of DC and B cells. FACS analysis of MHCII expression, that confers and modulates APC activity (12), revealed that ovx increases the frequency of MHCII-expressing Mϕ by >2-fold (Fig. 1d, time 0). Furthermore, ovx increases MHCII induction by the physiological stimulant IFN-γ in Mϕ (Fig. 1d). In contrast, ovx has no effect on MHCII expression in B cells and DC (data not shown). Together, these findings indicate that ovx enhances activation-induced T cell proliferation by increasing Mϕ APC activity through augmented MHCII expression.

We then investigated how ovx down-regulates T cell apoptosis, a phenomenon that follows T cell activation and contributes to regulate the duration of the immune response. Lifespan of activated T cells is limited by apoptosis induced by membrane bound FasL, expressed by T cells in response to activation, through a mechanism mediated by the nuclear factor of activated T cells (NFAT). This apoptotic program is referred to as activation-induced cell death (AICD) (13). Stress such as γ-irradiation also induces FasL expression and apoptosis in T cells through a mechanism independent of NFAT (14). We found that ovx markedly decreases AICD, but not stress-induced apoptosis (Fig. 1e). In accordance with this observation, we found that ovx represses the expression of FasL induced by activation, but not that induced by irradiation (Fig. 1f), suggesting that ovx specifically blunts AICD by suppressing the activation-induced expression of FasL.

Altogether, these observations suggest that estrogen deficiency enhances T cell activation by potentiating APC activity in Mϕ, while extending the lifespan of active T cells by suppressing AICD. These alterations result in the expansion of the pool of active, TNF-producing T cells in the bone marrow, leading to chronic stimulation of osteoclast formation and bone loss. According to this hypothesis, the T cell expansion and the bone loss that follow ovx are dependent on T cell activation by APC.

APC Activity Is Required for Ovx-Induced T Cell Expansion and Bone Loss. To determine whether the increased T cell proliferation and lifespan induced by ovx require APC-T cell interaction *in vivo*, we used DO11.10 mice, a strain characterized by impaired MHCII-T cell receptor (TCR) interaction, caused by the presence of a single TCR specificity toward the foreign Ag chicken albumin (ovalbumin) (15). In DO11.10 mice, ovx fails to increase T cell proliferation and lifespan (Table 1). As a result, in these mice, ovx fails to increase the pool of TNF-producing T cells. Injection of ovalbumin in sham DO11.10 mice leads to an increase of both T cell proliferation and AICD, attributable to restoration of APC-T cell interaction, which results in a small ($\approx$0.5-fold) increase in the number of TNF producing T cells. In contrast, ovalbumin treatment restores the capacity of ovx to expand the pool of TNF-producing T cells by $\approx$3-fold by further increasing proliferation and by blunting T cell apoptosis. These data demonstrate that APC activity is critical in the process by which ovx increases T cell proliferation and lifespan, leading to increased T cell number.

To assess the relevance *in vivo* of APC-T cell interaction in ovx-induced bone loss, BMD was measured *in vivo* in DO11.10 mice and WT controls of identical genetic background before
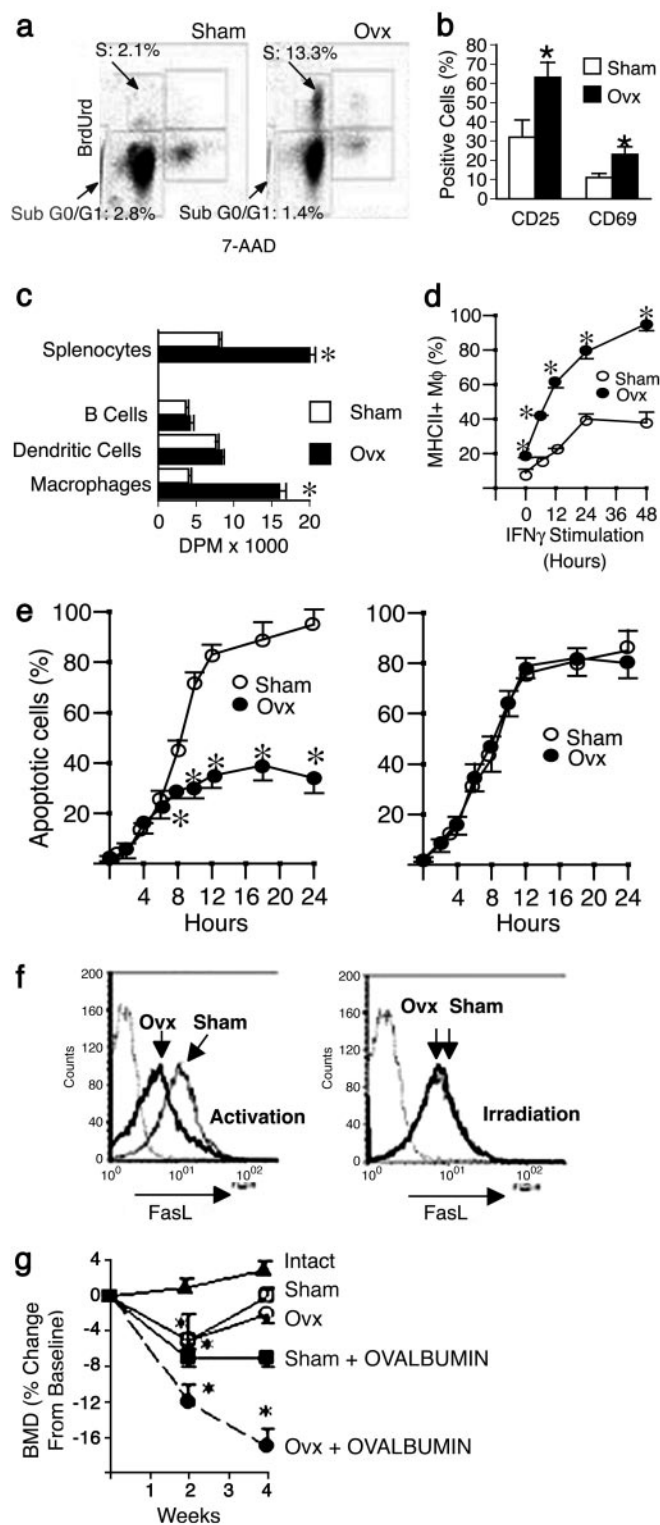
Fig. 1. *In vivo* analysis of T cell proliferation, apoptosis, and Ag presentation in ovx mice. (*a*) Analysis of BrdUrd incorporation and total DNA content (7-amino-actinomycin, 7-AAD) in spleen CD3+ T cells from sham-operated mice (*Left*) and ovx mice (*Right*). Proliferation is indicated as percentage of T cells in S phase. Percentage of apoptotic T cells is represented by the population in SubG_0/G_1 phase. (*b*) FACS analysis of T cell activation in the bone marrow. Data are expressed as percentage (mean ± SEM) of CD3+ T cells expressing CD25 or CD69. (*c*) APC activity of spleen cells and purified subpopulations of professional APCs from sham and ovx mice, as assessed by incorporation of [³H]thymidine by target T cells (data expressed as mean ± SEM of disintegrations per minute). (*d*) FACS analysis of MHCII expression in

peritoneal Mϕ from sham and ovx mice. Data are expressed as percentage (mean ± SEM) of Mϕ expressing MHCII. (*e*) FACS analysis of activation- and irradiation-induced apoptosis in spleen CD4+ T cells. Data are expressed as percentage (mean ± SEM) of live apoptotic cells assessed by binding of annexin V. (*f*) FACS analysis of activation- and irradiation-induced FasL expression in spleen CD4+ T cells. Isotype control is indicated by the dotted line. All data are representative of at least three independent experiments. *, $P < 0.05$ compared with the corresponding sham group. (*g*) *In vivo* role of Ag presentation in ovx-induced bone loss. Shown is the effect of ovx on femoral BMD of DO11.10 mice ($n = 6$ per group). Data are expressed as percentage change (mean ± SEM) from baseline. *, $P < 0.05$ compared with both baseline and intact mice.

surgery and 2 and 4 weeks after either ovx or sham operation. In WT mice, ovx but not sham operation induced rapid bone loss (ovx: −7.7 ± 1.4%, $P < 0.05$; sham +2.64 ± 0.8%, $P =$ not significant, compared with baseline). Sham and ovx DO11.10 mice sustained an equal, small bone loss during the first 2 weeks, presumably representing a sex steroid-independent response to surgical stress (Fig. 1g), followed by return to baseline at 4 weeks from surgery. Thus, DO11.10 mice are protected against ovx-induced bone loss. In sham DO11.10 mice, treatment with ovalbumin was followed by a significant bone loss, attributable to the immune reaction to the Ag in the context of unstimulated APC activity (15). In ovx DO11.10 mice, treatment with ovalbumin caused a significantly larger bone loss reflecting the cumulative effects of Ag stimulation and ovx-induced increased APC activity. Thus, in parallel with T cell expansion, treatment with ovalbumin restores the ability of ovx to induce bone loss in DO11.10 mice. Together, these findings demonstrate that APC-induced T cell activation is critical in the process by which ovx increases T cell number, and ultimately leads to bone loss.

Ovx Increases CIITA in APCs and T Cells Through Augmented IFN-γ. We then investigated how ovx increases APC activity and decreases AICD. CIITA is the master regulator of MHCII expression and APC activity (12). Furthermore, CIITA expression in T cells prevents activation-induced FasL expression and apoptosis *in vitro* (16) and *in vivo* (17). Thus, increased CIITA levels in Mϕ and T cells could mediate both the stimulatory effect on APC activity and the inhibitory effect on AICD induced by ovx. Indeed, reverse transcriptase real-time PCR analysis revealed 3-fold higher CIITA transcript levels in Mϕ and 2-fold higher levels in T cells from ovx mice, as compared with sham-operated controls (Fig. 2a), indicating that CIITA is regulated by estrogen *in vivo*. Unlike DC and B cells, in which CIITA is constitutively expressed, in Mϕ and T cells, CIITA expression is transcriptionally regulated, and specifically induced by IFN-γ (12, 18). To test whether increased CIITA in ovx mice requires IFN-γ signaling, we used IFN-γR$^{-/-}$ mice. In striking opposition to what observed in WT mice, ovx of IFN-γR$^{-/-}$ mice of identical genetic background fails to up-regulate CIITA in Mϕ and T cells, demonstrating that CIITA up-regulation by ovx is mediated by IFN-γ. We thus hypothesized that ovx increases CIITA *in vivo* by increasing the production of IFN-γ. This cytokine is produced mainly by CD4+ T$_H$ cells on differentiation into T$_H$1 cells (19). FACS analysis demonstrated that ovx enhances IFN-γ production by T$_H$ cells in the BM, and also in secondary lymphoid organs, such as lymph nodes (Fig. 2b) and spleen (not shown). No effect of ovx on IFN-γ production by natural killer (NK) cells, another potential source of this cytokine (20), was detected by FACS (not shown). Thus, ovx specifically up-regulates T$_H$1 IFN-γ production *in vivo*, despite reports that estrogen exerts a direct stimulatory effect on IFN-γ gene expression *in vitro* (21).

Measurements by ELISA confirmed that purified, unstimulated T$_H$ cells derived from ovx mice secrete detectable amounts of IFN-γ, whereas IFN-γ is undetectable in culture supernatants

MEDICAL SCIENCES

Table 1. *In vivo* role of Ag presentation in ovx-induced T cell expansion

	T cells in S phase, % of T cells	T cells in sub-G_0/G_1 phase, % of T cells	TNF-producing T cells, % of BM white cells
DO11.10 sham	2.23 ± 0.4	0.56 ± 0.2	0.43 ± 0.1
DO11.10 ovx	1.87 ± 0.7	0.78 ± 0.4	0.32 ± 0.1
DO11.10 sham + ovalbumin	4.4 ± 0.5*	1.6 ± 0.2*	0.67 ± 0.2
DO11.10 ovx + ovalbumin	14.1 ± 2.6*[†]	0.7 ± 0.1[†]	1.8 ± 0.4*[†]

Ovx fails to increase T cell proliferation (cells in S phase), to decrease T cell apoptosis (cells in sub-G_0/G_1 phase), and to increase BM T cells in DO11.10 mice (mean $\pm$ SEM).
*$P < 0.05$ as compared to untreated shams.
[†]$P < 0.05$ as compared to ovalbumin-treated shams.

of T_H cells from sham controls (Fig. 2c). IFN-γ production by T_H1 cells is induced by either a cyclosporin A-sensitive TCR-dependent mechanism, mediated by T cell activation, or by the cytokines IL-12 and IL-18 through activation of the mitogen-activated protein kinase p38 (19, 22). Increased production of IFN-γ by T_H cells from ovx mice is suppressed by *in vitro* treatment with the selective p38 inhibitor SB203580, but not by the activation inhibitor cyclosporin A, suggesting that increased IFN-γ production by T_H cells in ovx mice is cytokine-driven.

The expression of IL-12 and IL-18 genes in Mϕ is induced by NF-κB and AP-1 (23, 24), nuclear proteins whose transcriptional activity is directly repressed by estrogen in Mϕ (25–27). Unstimulated Mϕ, such as those from estrogen-replete mice, are known to express low or undetectable levels of NFkB and AP-1 (26, 28). In keeping with these observations, we found that sham Mϕ express undetectable levels of IL-12 and IL-18. Furthermore, ovx increases secretion of IL-12 and IL-18 by BM Mϕ, whereas *in vitro* treatment with 17β estradiol represses it (Fig. 2d). Thus, one mechanism by which ovx may increase CIITA expression is stimulation of IFN-γ secretion via enhanced Mϕ production of the IFN-γ-inducing cytokines IL-12 and IL-18.

IFN-γR$^{-/-}$ Mice Are Protected from Ovx-Induced Immune Alterations, T Cell Expansion, and Bone Loss. We then used IFN-γR$^{-/-}$ mice to assess the relevance *in vivo* of IFN-γ-induced CIITA in ovx-induced T cell expansion and bone loss. Neither basal nor IFN-γ-induced MHCII expression by Mϕ are increased by ovx in IFN-γR$^{-/-}$ mice (Fig. 3a). Furthermore, ovx fails to suppress AICD in T cells derived from IFN-γR$^{-/-}$ mice (Fig. 3b). The inability of ovx to increase T cell proliferation and to decrease T cell apoptosis in IFN-γR$^{-/-}$ mice was confirmed *in vivo* by BrdUrd incorporation analysis (Table 2). Importantly, ovx of IFN-γR$^{-/-}$ mice, but not of WT littermates, fails to increase the number of BM T cells and TNF-producing T cells *in vivo*, as assessed by FACS (Table 2), and T cell TNF and IFN-γ production *in vitro*, as assessed by ELISA (Fig. 3 c and d). To determine whether IFN-γ signaling mediates ovx-induced bone loss, BMD was measured *in vivo* in IFN-γR$^{-/-}$ mice and WT controls before surgery and 2 and 4 weeks after either ovx or sham operation. Before surgery, BMD was identical in WT and null mice (data not shown), demonstrating that IFN-γ signaling plays no role in skeletal development. At 4 weeks from ovx, BMD was significantly lower (Fig. 3e) than at baseline in WT mice (−8.0%), but not in IFN-γR$^{-/-}$ mice (−2.6%). Histological analysis of long bones confirmed that the loss of trabeculae induced by ovx in WT mice is absent in IFN-γR$^{-/-}$ mice (Fig. 3f). Together, our *in vivo* studies demonstrate that ovx causes T cell expansion and bone loss through APC-induced T cell activation and IFN-γ signaling, via induction of the critical mediator CIITA.

Discussion

This study confirms that ovx-induced bone loss depends on the ability of estrogen deficiency to expand the number of TNF producing T cells. Furthermore, the data demonstrate that *in vivo* estrogen deficiency causes T cell expansion by enhancing T cell proliferation and lifespan. Both phenomena result from IFN-γ-mediated induction of CIITA in Mϕ and T cells. Increased CIITA expression leads to augmented Ag presentation by Mϕ, enhanced T cell activation, and increased activation-dependent proliferation and lifespan of active T cells (Fig. 4, which is published as supporting information on the PNAS web site, www.pnas.org).

A previously unknown, multifaceted role of IFN-γ as regulator of bone homeostasis is disclosed. IFN-γ is known to exert a direct anti-osteoclastogenic activity *in vitro* and to mitigate infection-induced bone loss by inhibiting RANKL-induced osteoclastogenesis (29, 30). Surprisingly, our findings reveal that in conditions of estrogen deficiency, IFN-γ-driven induction of CIITA leads to increased APC activity, T cell proliferation, and lifespan, events that ultimately lead to expansion of the T cell pool, enhanced T cell TNF production, and TNF-induced bone loss *in vivo* (4, 6, 7). Thus, despite its bone-sparing effects in some conditions, such as infection-induced bone loss, IFN-γ is a critical enhancer of the bone loss induced by estrogen deficiency.

As to the mechanism of CIITA induction in ovx mice, our findings demonstrate the essential role of cytokine driven stimulation of IFN-γ production and signaling. Importantly, because CIITA expression in T cells stimulates IFN-γ production (18), and IFN-γ stimulates both its own inducers, IL-18 and IL-12, and IL-12 receptor expression (19, 24), ovx triggers an amplification loop leading to a further increase in the level of IFN-γ and the resulting induction of CIITA. The observation that ovx fails to increase IFN-γ levels in IFN-γR$^{-/-}$ mice confirms that increased IFN-γ results primarily from IFN-γ-induced events such as IL-12 and IL-18 signaling, and CIITA expression (19, 24).

An increased responsiveness of CIITA to IFN-γ, disclosed by the higher MHCII expression in ovx than in sham Mϕ in response to IFN-γ, may contribute to increase CIITA levels in conditions of estrogen deficiency. Such increased responsiveness of ovx Mϕ to IFN-γ is likely to be related to a priming effect induced by the high bone marrow level of IFN-γ characteristic of ovx mice. Indeed, such phenomenon can be duplicated *in vitro* by the prolonged stimulation of sham Mϕ with the level of IFN-γ measured in the bone marrow of ovx mice (data not shown).

The results of this study and of previous reports pointing to a causal role of TNF in ovx-induced bone loss are not in contrast with published evidence demonstrating the relevance of other estrogen-regulated cytokines such as IL-1, IL-6, macrophage colony-stimulating factor, and OPG (5). For example, the report that ovx fails to induce bone loss in TNF$^{-/-}$ mice (7) is not in conflict with studies demonstrating that mice lacking IL-6 (31) or IL-1R (32) are also protected against ovx induced bone loss. Cytokines are, in fact, under reciprocal control and organized in a cascade fashion. Thus, blockade of either upstream or downstream factors of the same cascade is effective in preventing bone loss in ovx mice. Furthermore, cytokines are recognized for their synergistic interactions. Thus, the neutralization of a single factor may achieve the same
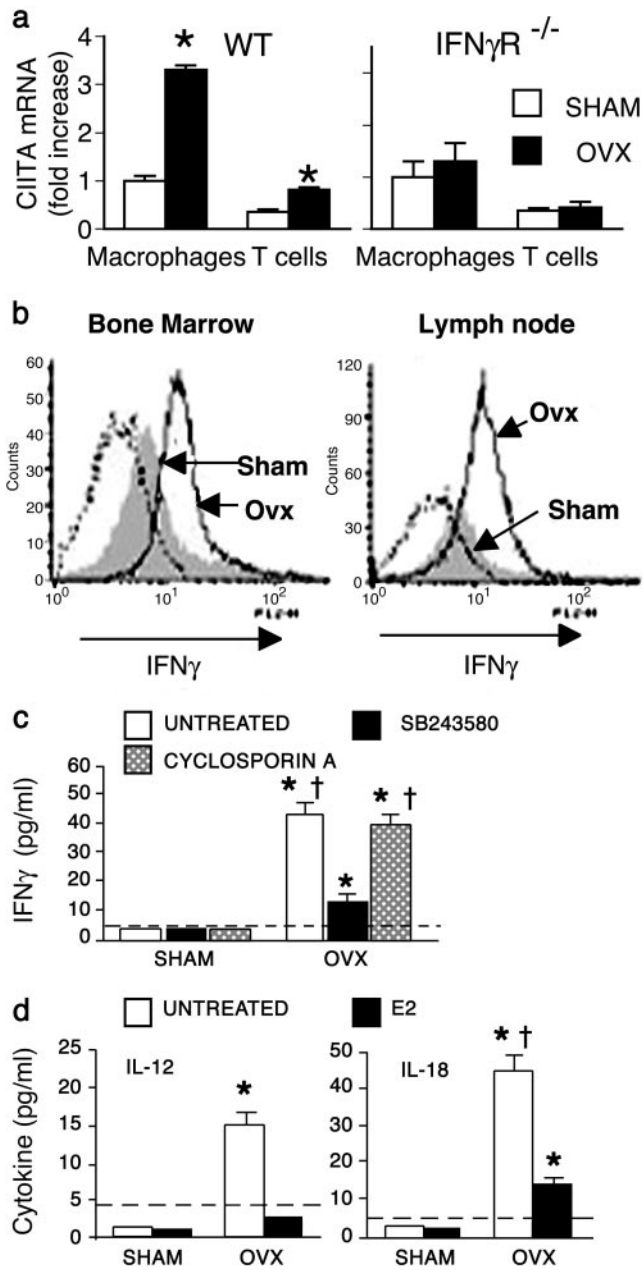
Fig. 2. Ovx increases IFN-γ-induced CIITA in APCs and T cells. (*a*) Reverse transcriptase real-time PCR analysis of CIITA mRNA levels in BM Mφ and T cells from WT and IFN-γR$^{-/-}$ mice of identical genetic background. (*b*) FACS analysis of IFN-γ levels in gated CD4$^+$ T cells in BM (*Left*), and lymph nodes (*Right*) from sham and ovx mice. Isotype control is indicated by the dotted line. (*c*) ELISA for IFN-γ concentration in culture supernatants of purified BM CD90+ T cells, unstimulated or treated with cyclosporin A or SB203580. Data are expressed as mean ± SEM of six replicates. ∗, $P < 0.05$ compared with all undetectable groups by Fisher exact test. †, $P < 0.05$ compared with ovx, SB203580-treated groups. The dashed line indicates assay detection threshold. (*d*) ELISA for IL-12 and IL-18 levels in culture supernatants of purified CD11b+ BM Mφ, treated with 17β estradiol (E2) or left untreated. Data are expressed as mean ± SEM of six replicates. ∗, $P < 0.05$ compared with all undetectable groups by Fisher exact test. †, $P < 0.05$ compared with ovx, E2-treated groups. The dashed line indicates assay detection threshold. All data are representative of at least three independent experiments.

effect as the neutralization of the sister cytokine or both factors. Examples are the well defined synergies between IL-1 and TNF (33), and TNF and RANKL (4).
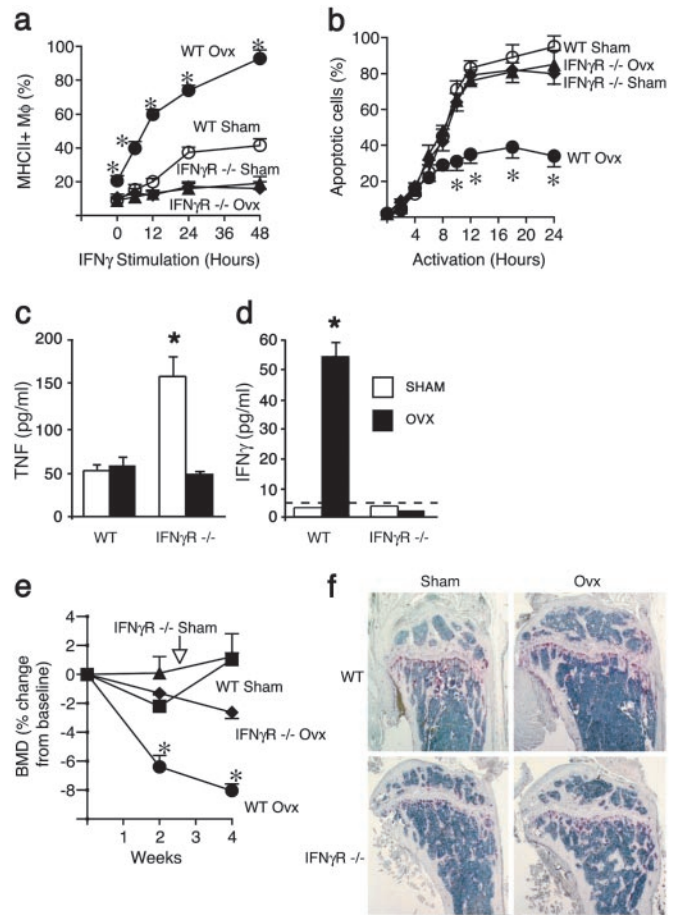

Fig. 3. IFN-γR$^{-/-}$ mice are protected from ovx-induced immune alterations, T cell expansion, and bone loss. (*a*) Basal and IFN-γ-stimulated MHCII expression by Mφ from sham and ovx WT and IFN-γR$^{-/-}$ mice. Data are expressed as percentage (mean ± SEM) of Mφ expressing MHCII. (*b*) FACS analysis of AICD in T$_H$ cells from sham and ovx WT and IFN-γR$^{-/-}$ mice. Percentage (mean ± SEM) of live apoptotic cells assessed by binding of annexin V is shown. All data are representative of at least three independent experiments. (*c* and *d*) Levels of TNF and IFN-γ in supernatants from purified unstimulated T$_H$ cells from sham and ovx WT and IFN-γR$^{-/-}$ mice. Data are expressed as average (±SEM) of six replicate samples. ∗, $P < 0.05$ compared with all other groups. The dashed line indicates assay detection threshold. (*e*) Analysis of BMD in sham and ovx WT and IFN-γR$^{-/-}$ mice ($n = 6$ per group). Data are expressed as percentage change (mean ± SEM) from baseline. ∗, $P < 0.05$ compared with baseline. (*f*) Histology of proximal tibia of sham and ovx WT and IFN-γR$^{-/-}$ mice. Representative samples from one mouse per group are shown. WT ovx mice, but not IFN-γR$^{-/-}$ mice, exhibit decreased trabecular bone and increased tartrate-resistant acid phosphatase positive osteoclasts (red staining) as compared with sham controls.

The current study provides evidence a novel regulatory link between the immune system and bone homeostasis, and contributes to elucidate the immune targets of estrogen deficiency. Interestingly, although our findings demonstrate that estrogen represses T$_H$1 activity and T cell production of the key inflammatory cytokine TNF, previous reports have shown immunostimulatory effects of estrogen (34). These apparently conflicting observations underscore the complex effects of sex steroids on immunity. This complexity is caused by the effects of estrogen on other immunoregulatory hormones such as prolactin and progesterone (35), the ability to regulate both pro- and antiinflammatory cytokines, and the capacity to exert relevant extra-immunological effects. Our findings are in accordance with clinical observations suggesting that in general estrogen stimu-

Table 2. IFNγR$^{-/-}$ mice are protected from ovx-induced T cell expansion

	T cells in S phase, %	T cells in sub-G0/G1 phase, %	T cells, % of BM white cells	TNF-producing T cells, % of BM white cells
WT sham	2.3 ± 0.2	2.8 ± 0.4	4.51 ± 0.35	0.97 ± 0.15
WT ovx	9.9 ± 0.4*	1.1 ± 0.3*	8.39 ± 0.59*	2.35 ± 0.49*
IFNγR$^{-/-}$ sham	3.1 ± 0.3	2.5 ± 0.3	2.79 ± 0.24	1.16 ± 0.16
IFNγR$^{-/-}$ ovx	2.2 ± 0.1	2.8 ± 0.2	2.72 ± 0.43	0.94 ± 0.14

Ovx fails to increase T cell proliferation (cells in S phase), to decrease T cell apoptosis (cells in sub-G_0/G_1 phase), and to increase BM T cells in IFNγR$^{-/-}$ mice (mean ± SEM).
*$P < 0.05$ as compared to all other groups.

lates T_H2 cytokine production and the humoral immune response, whereas it represses T_H1 behavior and cell-mediated immunity (5, 34–36). In keeping with this hypothesis, rheumatoid arthritis and multiple sclerosis, cell-mediated T_H1-dependent autoimmune diseases, are relieved during pregnancy and are exacerbated in postpartum, whereas the opposite relationship is observed in systemic lupus erythematosus, an immune complex-mediated autoimmune disease (5, 37–39).

In conclusion, not only may our findings contribute to explain why bone loss is commonly associated with inflammation and infection (40, 41), but, should these findings be confirmed in humans, postmenopausal osteoporosis could be regarded as a disease stemming from an inappropriate immune response, triggered by estrogen deficiency. Thus, recognition of the immune targets of estrogen *in vivo* may lead to identification of new therapeutic interventions not only for osteoporosis, but also for autoimmune and inflammatory conditions.

1. Riggs, B. L., Khosla, S. & Melton, L. J., III (2002) *Endocr. Rev.* **23,** 279–302.
2. Kousteni, S., Chen, J. R., Bellido, T., Han, L., Ali, A. A., O'Brien, C. A., Plotkin, L., Fu, Q., Mancino, A. T., Wen, Y., *et al.* (2002) *Science* **298,** 843–846.
3. Riggs, B. L. (2000) *J. Clin. Invest.* **106,** 1203–1204.
4. Lam, J., Takeshita, S., Barker, J. E., Kanagawa, O., Ross, F. P. & Teitelbaum, S. L. (2000) *J. Clin. Invest.* **106,** 1481–1488.
5. Pfeilschifter, J., Koditz, R., Pfohl, M. & Schatz, H. (2002) *Endocr. Rev.* **23,** 90–119.
6. Cenci, S., Weitzmann, M. N., Roggia, C., Namba, N., Novack, D., Woodring, J. & Pacifici, R. (2000) *J. Clin. Invest.* **106,** 1229–1237.
7. Roggia, C., Gao, Y., Cenci, S., Weitzmann, M. N., Toraldo, G., Isaia, G. & Pacifici, R. (2001) *Proc. Natl. Acad. Sci. USA* **98,** 13960–13965.
8. Cenci, S., Weitzmann, M. N., Gentile, M. A., Aisa, M. C. & Pacifici, R. (2000) *J. Clin. Invest.* **105,** 1279–1287.
9. Garside, P., Ingulli, E., Merica, R. R., Johnson, J. G., Noelle, R. J. & Jenkins, M. K. (1998) *Science* **281,** 96–99.
10. Kanagawa, O., Xu, G., Tevaarwerk, A. & Vaupel, B. A. (2000) *J. Immunol.* **164,** 3919–3923.
11. Weitzmann, M. N., Cenci, S., Rifas, L., Brown, C. & Pacifici, R. (2000) *Blood* **96,** 1873–1878.
12. Reith, W. & Mach, B. (2001) *Annu. Rev. Immunol.* **19,** 331–373.
13. Krammer, P. H. (2000) *Nature* **407,** 789–795.
14. Faris, M., Latinis, K. M., Kempiak, S. J., Koretzky, G. A. & Nel, A. (1998) *Mol. Cell. Biol.* **18,** 5414–5424.
15. Murphy, K. M., Heimberger, A. B. & Loh, D. Y. (1990) *Science* **250,** 1720–1723.
16. Gourley, T. S. & Chang, C. H. (2001) *J. Immunol.* **166,** 2917–2921.
17. Gourley, T. S., Patel, D. R., Nickerson, K., Hong, S. C. & Chang, C. H. (2002) *J. Immunol.* **168,** 4414–4419.
18. Gourley, T., Roys, S., Lukacs, N. W., Kunkel, S. L., Flavell, R. A. & Chang, C. H. (1999) *Immunity* **10,** 377–386.
19. Murphy, K. M., Ouyang, W., Farrar, J. D., Yang, J., Ranganath, S., Asnagli, H., Afkarian, M. & Murphy, T. L. (2000) *Annu. Rev. Immunol.* **18,** 451–494.
20. Biron, C. A., Nguyen, K. B., Pien, G. C., Cousens, L. P. & Salazar-Mather, T. P. (1999) *Annu. Rev. Immunol.* **17,** 189–220.
21. Fox, H. S., Bond, B. L. & Parslow, T. G. (1991) *J. Immunol.* **146,** 4362–4367.
22. Yang, J., Zhu, H., Murphy, T. L., Ouyang, W. & Murphy, K. M. (2001) *Nat. Immunol.* **2,** 157–164.
23. Becker, C., Wirtz, S., Ma, X., Blessing, M., Galle, P. R. & Neurath, M. F. (2001) *J. Immunol.* **167,** 2608–2618.
24. Kim, Y. M., Im, J. Y., Han, S. H., Kang, H. S. & Choi, I. (2000) *J. Immunol.* **165,** 3198–3205.
25. An, J., Ribeiro, R. C., Webb, P., Gustafsson, J. A., Kushner, P. J., Baxter, J. D. & Leitman, D. C. (1999) *Proc. Natl. Acad. Sci. USA* **96,** 15161–15166.
26. Shevde, N. K., Bendixen, A. C., Dienger, K. M. & Pike, J. W. (2000) *Proc. Natl. Acad. Sci. USA* **97,** 7829–7834.
27. Galien, R. & Garcia, T. (1997) *Nucleic Acids Res.* **25,** 2424–2429.
28. Muegge, K. & Durum, S. (1990) *Cytokine* **2,** 1–8.
29. Takayanagi, H., Ogasawara, K., Hida, S., Chiba, T., Murata, S., Sato, K., Takaoka, A., Yokochi, T., Oda, H., Tanaka, K., *et al.* (2000) *Nature* **408,** 600–605.
30. Kamolmatyakul, S., Chen, W. & Li, Y. P. (2001) *J. Dent. Res.* **80,** 351–355.
31. Poli, V., Balena, R., Fattori, E., Markatos, A., Yamamoto, M., Tanaka, H., Ciliberto, G., Rodan, G. A. & Costantini, F. (1994) *EMBO J.* **13,** 1189–1196.
32. Lorenzo, J. A., Naprta, A., Rao, Y., Alander, C., Glaccum, M., Widmer, M., Gronowicz, G., Kalinowski, J. & Pilbeam, C. C. (1998) *Endocrinology* **139,** 3022–3025.
33. Dinarello, C. A., Okusawa, S. & Gelfand, J. A. (1989) *Prog. Clin. Biol. Res.* **299,** 203–215.
34. Cutolo, M., Seriolo, B., Villaggio, B., Pizzorni, C., Craviotto, C. & Sulli, A. (2002) *Ann. N.Y. Acad. Sci.* **966,** 131–142.
35. McMurray, R. W. (2001) *Int. Immunopharmacol.* **1,** 995–1008.
36. Burger, D. & Dayer, J. M. (2002) *Ann. N.Y. Acad. Sci.* **966,** 464–473.
37. Ito, A., Bebo, B. F., Jr., Matejuk, A., Zamora, A., Silverman, M., Fyfe-Johnson, A. & Offner, H. (2001) *J. Immunol.* **167,** 542–552.
38. Confavreux, C., Hutchinson, M., Hours, M. M., Cortinovis-Tourniaire, P. & Moreau, T. (1998) *N. Engl. J. Med.* **339,** 285–291.
39. Jansson, L. & Holmdahl, R. (1998) *Inflamm. Res.* **47,** 290–301.
40. Baker, P., Howe, L., Garneau, J. & Roopenian, D. (2002) *FEMS Immunol. Med. Microbiol* **34,** 45.
41. Romas, E., Gillespie, M. T. & Martin, T. J. (2002) *Bone* **30,** 340–346.